

# Molecular Imprinting of Maltose Binding Protein: Tuning Protein Recognition at the Molecular Level

Maya Zayats,<sup>†</sup> Manu Kanwar,<sup>‡</sup> Marc Ostermeier,<sup>‡,§</sup> and Peter C. Searson<sup>\*,†,§</sup>

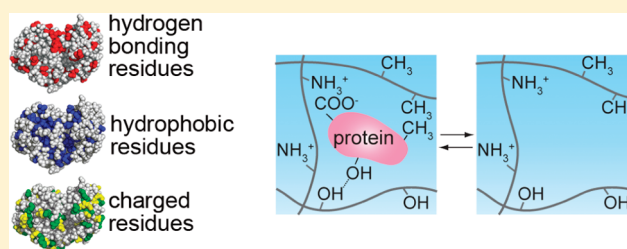
<sup>†</sup>Department of Materials Science and Engineering, Johns Hopkins University, Baltimore, Maryland 21218, United States

<sup>‡</sup>Department of Chemical and Biomolecular Engineering, Johns Hopkins University, Baltimore, Maryland 21218, United States

<sup>§</sup>Institute for NanoBioTechnology, Johns Hopkins University, Baltimore, Maryland 21218, United States

**S** Supporting Information

**ABSTRACT:** Protein imprinting in hydrogels is one approach for developing artificial receptors capable of specific recognition and binding of a target molecule. Through selection of monomers with side groups that can interact with the target protein and control over the degree of cross-linking, the architecture and spatial distribution of interaction points can be optimized for a target protein. Here we report on the imprinting of polyacrylamide-based hydrogels with maltose binding protein (MBP). To design the optimum architecture, we analyze the distribution of surface amino acid residues on the protein surface. We show that the selectivity of MBP recognition is increased by incorporating monomers that can introduce sites for hydrogen bonding, hydrophilic interactions, and electrostatic interactions. MBP-imprinted films showed high specificity and could discriminate between reference proteins with similar molecular weight, dimensions, and isoelectric point.



## INTRODUCTION

Molecularly imprinted polymers (MIPs) provide the means for designing and developing artificial receptors capable of specific recognition and binding of a target molecule.<sup>1–3</sup> Molecular imprinting is an approach that involves formation of a recognition site or binding pocket at the surface or inside a polymer matrix (e.g., thin film or particles) by incorporating functional monomers with side groups that can interact with the target molecule. After polymerization, the template molecule is removed from the polymeric matrix, leaving recognition sites that are complementary in shape, size, and spatial distribution of functional groups to the target. Because of their stability and low cost, molecularly imprinted polymers have been explored for applications in chromatography,<sup>4,5</sup> drug delivery,<sup>6–8</sup> targeting,<sup>9,10</sup> and sensors.<sup>11,12</sup>

Recognition of proteins using molecular imprinting is particularly challenging due to their size and structural complexity; however, there is growing interest in producing artificial antibodies for high throughput diagnostics and sensing.<sup>13–16</sup> Much of the work in this field has been based on the use of polyacrylamide hydrogels.<sup>17–21</sup> Polyacrylamide gels are widely used for protein separations and are biocompatible. Copolymers incorporating monomers with charged side groups have also been investigated.<sup>22–27</sup>

The key issue in designing polymers for protein imprinting is to find the optimum monomer composition that will interact with the target protein with high affinity. Side groups that introduce sites for hydrogen bonding, hydrophobic interactions,

and electrostatic interactions are most often investigated; however, experimentally, the monomers are usually selected empirically without any correlation to the protein structure. Here we present a study of protein imprinting based on analysis of the protein structure. Maltose binding protein (MBP) was selected as the template protein. MBP is a relatively small 41 kDa protein approximately  $3 \times 4 \times 6.5$  nm in size with surface residues capable of both hydrogen bonding interactions and hydrophobic interactions. MBP is negatively charged with a pI of 5.22 but has both positively and negatively charged surface residues. Through analysis of the surface residues we selected functional monomers to introduce hydrogen bonding, hydrophobic, and electrostatic interaction points into the protein recognition sites. The binding affinity of the template protein was characterized as a function of the composition of the hydrogel. We found that the optimal monomer composition for MBP imprinting contains 48% hydrogen bonding monomer (AAm), 48% hydrophobic monomer (NIPAm), 1% negatively charged monomer (MAA), and 1% positively charged monomer (DMAPMA).

## EXPERIMENTAL SECTION

**Materials.** *N*-Isopropylacrylamide (NIPAm), acrylamide (AAm), methacrylic acid (MAA), *N*-[3-(dimethylamino)propyl]methacrylamide

**Received:** February 15, 2011

**Revised:** April 12, 2011

**Published:** April 21, 2011

**Table 1. Composition of Polymer Films: (AAM) Acrylamide, (NIPAm) *N*-Isopropylacrylamide, (DMAPMA) *N*-[3-(Dimethylamino)propyl]methacrylamide, (MAA) Methacrylic Acid, and (MBA) *N,N*-Methylenebisacrylamide**

polymer	composition (mol %)				
	AAM	NIPAm	DMAPMA	MAA	MBA
1	98	0	0	0	2
2	78	20	0	0	2
3	49	49	0	0	2
4	20	78	0	0	2
5	0	98	0	0	2
6	48.5	48.5	1	0	2
7	48.5	48.5	0	1	2
8	48	48	1	1	2

(DMAPMA), *N,N*-methylenebis(acrylamide) (MBA), ammonium persulfate, *N,N,N',N''*-tetramethylenebis(acrylamide) (TEMED), 3-(trimethoxysilyl)propyl methacrylate, and Tris buffer were obtained from Sigma-Aldrich. Details of expression and purification of maltose binding protein (MBP) are provided in the Supporting Information. Bovine serum albumin (BSA) and ovalbumin (OVA) were obtained from Sigma. Proteinase K was purchased from New England BioLabs. All chemicals were used as received. All experiments were performed using ultrapure water (MilliPore).

**Preparation of Molecularly Imprinted Polymer (MIP) Films.** Microscope glass slides (1.5 cm × 1.5 cm, Fisher Scientific) were cleaned with piranha solution for 30 min, washed with deionized water, and dried under nitrogen. To improve polymer adhesion, the slides were modified by silanization. After incubation in 3-(trimethoxysilyl)propyl methacrylate (1%) in toluene overnight at room temperature, the slides were sequentially washed with toluene and water and then dried at 115 °C for 1 h. The silane-modified glass slides were stored under nitrogen at room temperature.

Freshly cleaved mica sheets (1.5 cm × 1.5 cm, grade V-4 from SPI Supplies) were used to ensure that the top surface of the polymer gels was flat. Each mica sheet was treated with silane to reduce adhesion to the gel and facilitate separation after gelation. Mica wafers were immersed in a solution of PlusOne Repel-Silane ES (GE Healthcare) for 10 min, sequentially washed with ethanol and water, and then air-dried.

The proteins MBP, BSA, and OVA were labeled with sulfoindocyanine *N*-hydroxysuccinimidyl ester dye (Cy3-NHS) (GE Healthcare, Amersham Cy3Mono-Reactive Dye Pack, PA23001) following procedures provided by the manufacturers. The average number of Cy3 molecules per protein molecule was 1, as determined by UV–vis spectroscopy. Although the Cy3 dye contains two negative charges and one positive charge, we assume that they do not influence rebinding since MBP has a large number of surface residues with positive and negatively charged side groups (see discussion below).

The precursor solution for producing the hydrogel films was prepared by mixing functional monomers (NIPAm, AAM, MAA, DMAPMA) along with a cross-linker (MBA) and ammonium persulfate (1 mg per 1 mL) in 10 mM Tris buffer (pH 7) to obtain a total monomer concentration of 10 wt %. In all cases the total amount of monomers (including cross-linker) was  $1.69 \times 10^{-3}$  mol. Subsequently, TEMED was added to initiate polymerization. The compositions studied here are summarized in Table 1.

As an example, a nonimprinted polymer with a 1:1 mole ratio of AAM and NIPAm monomers and 2 mol % cross-linker was prepared as follows. AAM ( $8.27 \times 10^{-4}$  mol), NIPAm ( $8.27 \times 10^{-4}$  mol), MBA ( $3.38 \times 10^{-5}$  mol), and ammonium persulfate (1 mg per 1 mL) were

mixed in a volume of 10 mM Tris buffer (pH 7) to obtain a total monomer concentration of 10 wt %. To initiate polymerization, 5  $\mu$ L of TEMED (6.5% v/v, aqueous solution) was added to 50  $\mu$ L of precursor solution and then immediately deposited on a silane-modified glass slide and covered by a mica wafer. The imprinted polymers (MIPs) were prepared in the same way by adding MBP labeled with Cy3 (MBP-Cy3) (1 mg mL<sup>-1</sup> in Tris buffer) to the precursor solution to achieve a final concentration of 0.5 mg mL<sup>-1</sup>. Polymerization was conducted at 35 °C for 3 h. After polymerization, the mica was removed from the surface of the polymer film on the glass slide by soaking in 10 mM Tris buffer solution pH 7 for 1.5 h. The buffer solution was analyzed by UV–vis spectroscopy to verify that no protein was removed from the polymer during mica separation. The thickness of all imprinted and nonimprinted films on the glass slides was about 100  $\mu$ m as measured by profilometer.

MBP-Cy3 was extracted from the polymer film by digestion with proteinase K (400  $\mu$ g mL<sup>-1</sup> in solution containing 100 mM NaCl and 50 mM CaCl<sub>2</sub>) for 12 h at 40 °C in the dark. The polymer films on the glass slides were then washed for 30 min in solution containing 10 mM Tris buffer and 500 mM NaCl to remove the protein fragments and proteinase K, followed by rinsing with 10 mM Tris buffer to remove NaCl. Nonimprinted polymers were subjected to the same treatment to avoid any differences in comparing to the imprinted polymers. Protein extraction is important since entrapped proteins influence the rebinding of the imprinted polymers. Proteinase K was selected for its lack of specificity in cleaving peptide bonds and its ability to break down proteins to very short peptides.<sup>28</sup> Protein removal by incubation in 10% SDS (w/v) in 10% (v/v) acetic acid,<sup>26,29</sup> 5 M urea, digestion with trypsin and Pronase E did not result in efficient extraction of MBP from the polymer films.

The affinity of the hydrogel films for the template protein was verified by rebinding experiments in which imprinted (MIP) and non-imprinted (NIP) films were incubated in 2.5 mL of MBP-Cy3 solution (0.5 mg mL<sup>-1</sup>) in Tris buffer pH 7 for 7 h at room temperature in the dark. The slides were then rinsed with the same buffer prior to measuring the fluorescence intensity of the films. The same experimental conditions were used during binding of BSA-Cy3 and OVA-Cy3 to polymers imprinted with MBP-Cy3.

The degree of hydration of the hydrogels was determined from gravimetric measurements of nonimprinted polymers (NIPs) before and after hydration. A fixed volume of precursor solution containing the monomers, cross-linker (MBA), and initiators (ammonium persulfate and TEMED) was placed on a coverslip. After polymerization, the hydrogel was dried under vacuum for 24 h and then weighed. The hydrogel was then incubated in 10 mM Tris buffer pH 7 for 7 h at room temperature in the dark. After removing from the buffer solution, excess solution was removed, and the hydrogel sample weighed. The swelling ratio (SR) was determined from  $(w_s - w_d)/w_d$  where  $w_s$  and  $w_d$  are the weight of the hydrated and dehydrated polymer, respectively.

After each step (protein imprinting, protein extraction, and protein rebinding), the films were imaged by fluorescence microscopy using a Nikon Eclipse ME 600 epifluorescence microscope. IPLab software (Scanalytics) was used to acquire fluorescence images using a 10× objective (NA 0.3). Images were collected using a SpotRT 229044 camera with 2 × 2 binning yielding 1600 × 1200 pixels. For measuring Cy3 fluorescence (Ex 550 nm, Em 570 nm) we used a Nikon G-2A filter cube (Ex 510–560 nm, DM 565 nm, BA 590 nm). The fluorescence of the imprinted films was measured at 25 ms exposure, and fluorescence of the films after protein extraction and rebinding was measured at 100 ms exposure. The average fluorescence intensities (per pixel) of the polymer films were determined using IPLab software.

Quantitative analysis of protein incorporation into the films was achieved by measuring the average fluorescence intensity for known concentrations of MBP-Cy3. The average fluorescence intensity (per pixel) of different MBP-Cy3 concentrations (0–1 mg mL<sup>-1</sup>) was

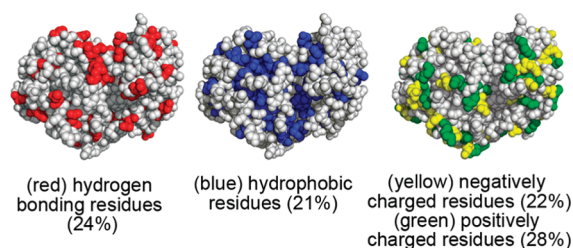


**Figure 1.** Distribution of amino acid residues on the surface of MBP.

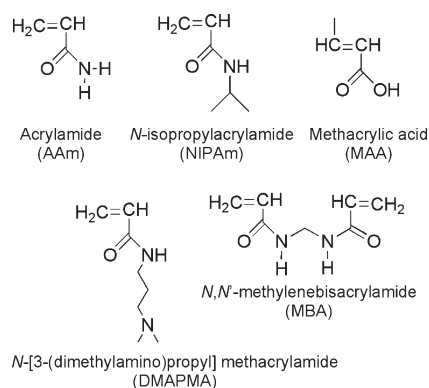


**Figure 2.** Molecular structure of the monomers used in this study.

determined by pipetting 5  $\mu\text{L}$  of the protein solution on a microscope slide and covering with a circular coverslip (1.13  $\text{cm}^2$ ) such that the solution was constrained to a fixed height and a fixed area. The fluorescence intensities were collected with exposure times of 25 and 100 ms and normalized to the intensity at 100 ms exposure for calibration.

The distribution of solvent-accessible residues on the MBP surface was analyzed using PISA (Protein Interfaces, Surfaces and Assemblies; [http://www.ebi.ac.uk/msd-srv/prot\\_int/pistart.html](http://www.ebi.ac.uk/msd-srv/prot_int/pistart.html), PDB ID 1anf).

## RESULTS AND DISCUSSION

Selective binding of a target protein is dependent on the composition of the functional monomers in the polymer gel. To guide selection of the functional monomers that provide the recognition elements for the protein, we analyzed the distribution of surface amino acid residues on MBP, based on their solvent accessible surface area. Figure 1 shows the distribution of hydrophobic, hydrogen bonding, negatively charged, and positively charged residues on the surface of MBP. About 24% of the surface residues are available for hydrogen bonding, and 21% have the potential to form hydrophobic interactions. Here we only consider the overall fraction of the residues, not the details of their distribution. The isoelectric point for MBP is 5.22, and hence the protein is negatively charged under physiological conditions. Nonetheless, 22% of the surface residues are negatively charged and 28% positively charged.

On the basis of the surface analysis, we selected the following monomers to provide interaction sites for the protein (Figure 2): *N*-isopropylacrylamide (NIPAm) to introduce sites for hydrophobic interaction, acrylamide (AAM) to introduce sites for hydrogen bonding interactions, the negatively charged monomer methacrylic acid (MAA), and the positively charged monomer *N*-[3-(dimethylamino)propyl] methacrylamide (DMAPMA). In a series of experiments, we have systematically varied the

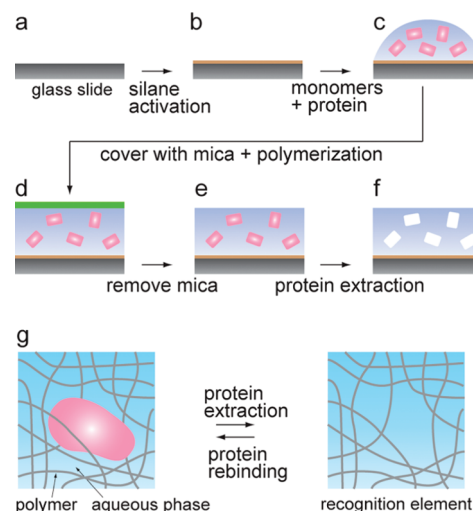


**Figure 3.** Schematic illustration of synthesis of imprinted polymer films. A glass slide (a) is modified with a 3-(trimethoxysilyl)propyl methacrylate silane (b) to improve adhesion of the polymer film. A fixed volume of precursor solution containing the monomers, cross-linker (MBA), initiators (ammonium persulfate and TEMED), and Cy3-labeled MBP (MBP-Cy3) was placed on a modified glass slide (c) and a mica wafer placed on top (d) prior to polymerization. Finally, the mica wafer is removed (e) and the protein extracted (f). (g) Protein extraction and rebinding.

monomer composition (Table 1) to study the relationship between the surface properties of the protein and the polymer composition and to determine the optimum composition to maximize binding selectivity.

Protein recognition was studied using bulk imprinting in hydrogel films. The steps involved in preparing the polymer films are illustrated in Figure 3a–f. Briefly, a fixed volume of precursor solution containing the monomers, cross-linker (MBA), initiators (ammonium persulfate and TEMED), and Cy3-labeled MBP (MBP-Cy3) was placed on a modified glass slide and covered by a mica wafer to ensure that the surface of the polymer is flat. After polymerization, the mica was removed and the protein extracted by digestion with proteinase K (Figure 3g). The affinity of the imprinted polymer films to MBP was determined through rebinding experiments.

We first studied recognition with AAM-based polymer films. In this case, the mechanism of recognition is due to hydrogen bonding between carbonyl and amide side groups on the polymer backbone (see Figure 2) and the surface accessible hydrophilic residues of the MBP that represent about 24% of the surface. Figure 4a shows fluorescence images of a nonimprinted film (NIP), an MBP-imprinted polymer film (MIP), and an imprinted film after digestion of the protein incorporated during film formation and subsequent exposure to MBP-Cy3 solution for 7 h. The imprinted film (MIP) shows bright fluorescence due to the incorporation of MBP-Cy3 (0.5  $\text{mg mL}^{-1}$ ) during film formation. After protein extraction, about 98% of the MBP-Cy3 was removed from the film. Rebinding experiments were performed by exposing these MBP-imprinted films to fresh MBP-Cy3 solution (0.5  $\text{mg mL}^{-1}$ ). The rebinding of MBP-Cy3 resulted in an increase in fluorescence compared to the imprinted film after protein extraction. The amount of protein in the film was determined quantitatively using fluorescence microscopy.

Figure 4b shows the fluorescence intensity versus MBP-Cy3 concentration in solution. From the calibration curve, we can convert the fluorescence intensity from the polymer films to a

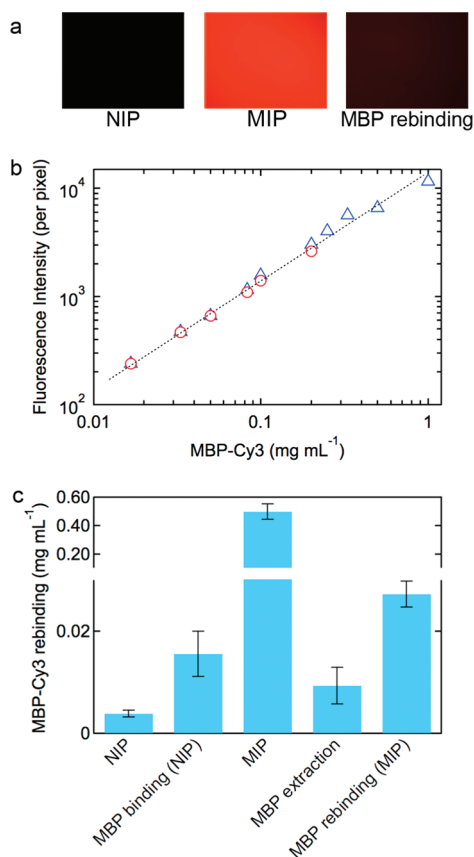


**Figure 4.** Protein recognition in polyacrylamide (pAAm) hydrogels. (a) Representative fluorescence images (1192  $\mu\text{m} \times 894 \mu\text{m}$ ) of a nonimprinted polymer (NIP), a polymer film after imprinting (MIP), and an imprinted film after protein extraction and rebinding (MBP rebinding). These images illustrate that protein incorporation, extraction, and rebinding are uniform. (b) Calibration curve of fluorescence intensity versus concentration of MBP-Cy3. Known concentrations of MBP-Cy3 were placed between two glass slides and the fluorescence intensity per pixel measured at different exposure times: ( $\Delta$ ) 25 ms and ( $\circ$ ) 100 ms. The fluorescence intensities were normalized to an exposure time of 100 ms. (c) Histogram showing protein incorporation at different steps during rebinding experiments: (NIP) autofluorescence of the nonimprinted polymer, (MBP binding (NIP)) protein uptake due to nonspecific binding in the nonimprinted polymer, (MIP) the amount of protein in the film after imprinting, (MBP extraction) amount of protein left in the imprinted film after protein extraction, (MBP rebinding (MIP)) amount of protein taken up by the imprinted film. Error bars represent the standard deviation for three independent experiments with different films.

protein concentration. Figure 4c shows results for rebinding MBP-Cy3 to imprinted and nonimprinted pAAm films. In our experiments, a protein concentration of 0.5 mg mL<sup>-1</sup> corresponds to  $7.3 \times 10^{13} \text{ cm}^{-2}$ .

From Figure 4c it is evident that the amount of protein taken up by the film after rebinding is about 5% of the amount of protein in the film after imprinting. The incubation time for rebinding was selected to ensure that the film was not saturated with the fluorescently labeled protein. The kinetics of protein uptake during rebinding are discussed in more detail below.

The ability of the imprinted polymers to bind the target protein was analyzed quantitatively from the imprinting

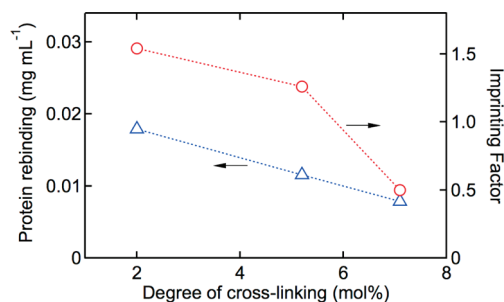


**Figure 5.** Influence of the degree of cross-linking on MBP-Cy3 rebinding to polyacrylamide (pAAm) imprinted film: ( $\circ$ ) imprinting factor versus degree of cross-linking; ( $\Delta$ ) amount of protein bound to the imprinted polymer film after protein extraction and rebinding.

factor, IF:

$$\text{IF} = \frac{m^{\text{IP}} - m_0^{\text{IP}}}{m^{\text{NIP}} - m_0^{\text{NIP}}} \quad (1)$$

where  $m^{\text{IP}}$  is the amount of MBP-Cy3 bound to the imprinted polymer,  $m^{\text{NIP}}$  is the amount of protein bound to the nonimprinted polymer,  $m_0^{\text{IP}}$  is the amount of MBP-Cy3 left in the imprinted polymer after extraction, and  $m_0^{\text{NIP}}$  is the intrinsic signal of the nonimprinted polymer. In most cases, the fluorescently labeled protein was completely removed from the polymer film and  $m_0^{\text{IP}} = m_0^{\text{NIP}}$ . Note that an imprinting factor of 1.0 corresponds to no selectivity to the target protein. From the results in Figure 4c, we determine an imprinting factor of 1.5 for MBP binding to pAAm.

The degree of cross-linking in the imprinted polymers plays an important role in protein recognition. Increasing cross-linking decreases the pore size and hence attenuates protein transport in the film. However, decreasing cross-linking increases the spatial fluctuations in the recognition sites and hence reduces binding efficiency. Figure 5 shows the amount of protein uptake and the imprinting factor for acrylamide-based gels with different degrees of cross-linking. The binding of MBP-Cy3 decreased with increasing cross-linking, indicating that we are in the regime where cross-linking controls protein transport. On the basis of these experiments, all other experiments were performed at 2 mol % cross-linking.

Next, we investigated protein imprinting in polymers with side groups for both hydrogen bonding and hydrophobic interactions by preparing gels with different amounts of AAm and NIPAm, a monomer with hydrophobic side groups (Table 1). Figure 6a shows results for rebinding MBP-Cy3 to imprinted and nonimprinted films with a 1:1 ratio of AAm and NIPAm. About 98% of the protein is removed from the imprinted polymer after digestion, and the increase in protein uptake on rebinding is significantly larger than for the nonimprinted polymer. Figure 6b shows the influence of the mole fraction of NIPAm in the polymer on protein recognition. The initial amount of protein in the AAm/NIPAm hydrogels and the amount remaining after extraction were the same, independent of composition. All AAm/NIPAm imprinted polymers showed measurable binding of MBP-Cy3, and the influence of polymer composition on imprinting factor is shown in Figure 6c. The imprinting factor increases from 1.5 for pure AAm to a value of 3.0 at a mole fraction of NIPAm of 0.49, suggesting that the hydrophobic side groups on the NIPAm introduce additional recognition sites and

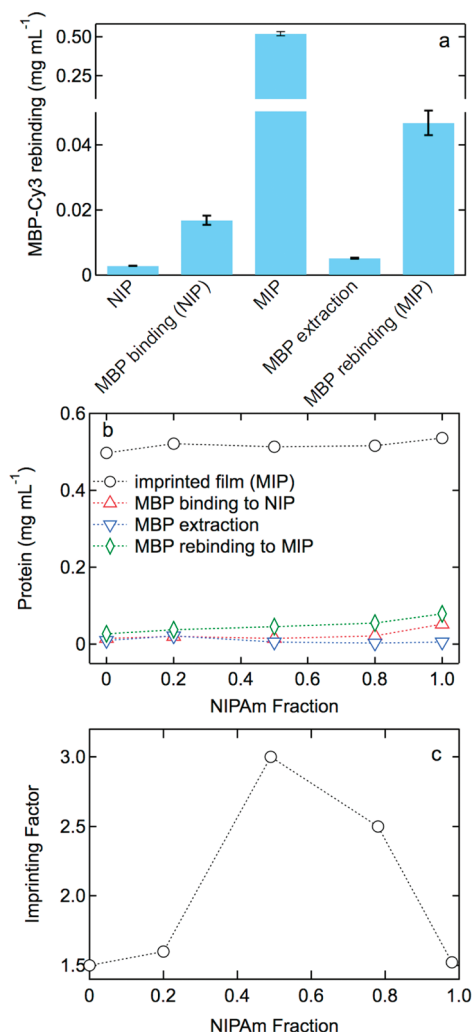


**Figure 6.** Protein recognition in AAm/NIPAm (49 mol %:49 mol %) hydrogels. (a) (NIP) autofluorescence of the nonimprinted polymer, (MBP binding (NIP)) protein uptake due to nonspecific binding in the nonimprinted polymer, (MIP) amount of protein in the film after imprinting, (MBP extraction) amount of protein left in the imprinted film after protein extraction, (MBP rebinding (MIP)) amount of protein taken up by the imprinted film. Error bars represent the standard deviation for three independent experiments with different films. (b) Protein concentration in the film versus composition. (○) Initial amount of MBP-Cy3 in the imprinted polymers, (▽) amount of MBP in the imprinted film after protein extraction, (△) amount of protein bound to the nonimprinted films due to nonspecific binding, (◇) amount of protein bound to the imprinted polymer film after protein extraction and rebinding. (c) Imprinting factor for MBP binding versus polymer composition in pAAm/pNIPAm films.

hence increase the imprinting factor. The peak in the imprinting factor at a mole fraction of 0.49 is very close to the fraction of hydrophobic surface residues of 0.47, taking into account only the hydrophobic and hydrophilic residues. Increasing the mole fraction of NIPAm higher than 0.49 results in a progressive decrease in imprinting factor, with a value of 1.5 for pure NIPAm.

The kinetics of protein recognition was determined by measuring MBP uptake with time for an AAm/NIPAm (49:49 mol %) polymer film. Figure 7 shows a plot of the integrated amount of protein in the film  $M$  plotted versus  $t^{1/2}$ . The linear behavior indicates that protein uptake in the imprinted film is

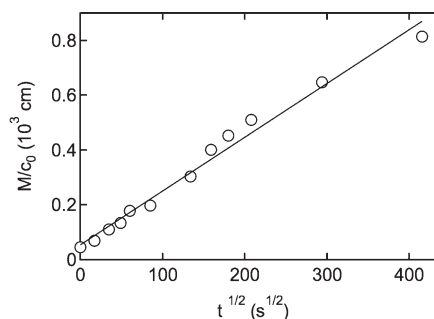


**Figure 7.** Amount of protein taken up by the imprinted polymer film plotted as  $M/c_0$  vs  $t^{1/2}$  for an AAm/NIPAm (49:49 mol %) polymer film.  $M$  is the amount of protein taken up by the polymer film (molecules cm<sup>-2</sup>) and  $c_0$  is the protein concentration in solution during rebinding (molecules cm<sup>-3</sup>). At  $t = 0$ , the initial concentration represents the protein not removed during digestion.

dominated by diffusion. Assuming a constant concentration of protein in the bulk solution, the total amount of protein taken up by the imprinted polymer film is given by<sup>30</sup>

$$\frac{M}{c_0} = 2 \left( \frac{Dt}{\pi} \right)^{1/2} \quad (2)$$

where  $D$  is the diffusion coefficient (cm<sup>2</sup> s<sup>-1</sup>),  $c_0$  is the protein concentration in solution during rebinding (molecules cm<sup>-3</sup>), and  $M$  is the amount of protein taken up by the polymer film (molecules cm<sup>-2</sup>). From a least-squares fit to the data, we obtain a diffusion coefficient of  $3.1 \times 10^{-12}$  cm<sup>2</sup> s<sup>-1</sup>. Thus, diffusion in the hydrogel films with 2% cross-linking is about 4 orders of magnitude slower than in aqueous solution where the diffusion coefficient is about  $5 \times 10^{-7}$  cm<sup>2</sup> s<sup>-1</sup>.<sup>31</sup> For the rebinding experiments reported here, the films were exposed to the target protein for 7 h. The diffusion length for the 7 h exposure time used in rebinding experiments is about 6  $\mu$ m, corresponding to a small fraction of the film.

PolyNIPAm is a thermosensitive hydrogel with a low critical solution temperature (LCST) of about 32 °C.<sup>32</sup> At temperatures below the critical temperature polyNIPAm absorbs water and exists in a swollen state, whereas above the critical temperature water is expelled and the hydrogel density increases significantly. The critical temperature can be controlled by adjusting the relative hydrophobicity. Thus, for AAm/NIPAm polymers, the critical temperature is increased by incorporation of the more hydrophilic AAm monomer.<sup>33,34</sup> We verified that there was no change in volume or optical transparency for all AAm/NIPAm films during polymerization (35 °C) or protein digestion (40 °C). The 98 mol % NIPAm films were opaque after polymerization, indicating a transition to the high density state. However, this did not appear to have significant influence on protein digestion or subsequent protein uptake in nonimprinted or imprinted polymers (see Figure 6b).

We next investigated the influence of electrostatic interactions on protein recognition in MBP imprinted polymers by incorporating monomers with charged side groups into the films. MBP is negatively charged at neutral pH (pI 5.22) but has approximately 22% negatively charged residues and 28% positively charged residues at the surface. In these experiments, we used a 1:1 mole ratio of AAm and NIPAm to maintain equal amounts of hydrophilic and hydrophobic residues.

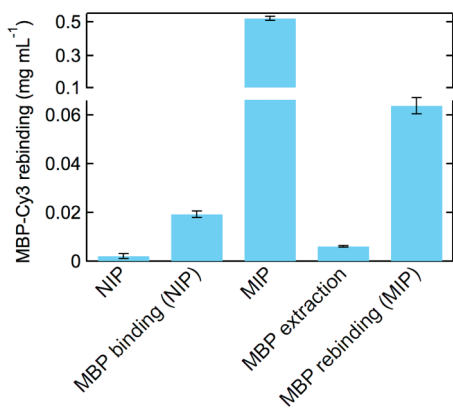


**Figure 8.** Protein recognition in AAm/NIPAm/DMAPMA/MAA hydrogels (48%:48%:1%:1%) comparing the amount of protein in non-imprinted and imprinted films. (NIP) autofluorescence in the non-imprinted polymer, (MBP binding (NIP)) protein uptake due to nonspecific binding, (MIP) amount of protein in the film after imprinting, (MBP extraction) amount of protein left in the imprinted film after protein extraction, (MBP rebinding (MIP)) amount of protein taken up by the imprinted film. Error bars represent the standard deviation for three independent experiments with different films.

The incorporation of 1 mol % of the positively charged monomer *N*-[3-(dimethylamino)propyl]methacrylamide (DMAPMA) with AAm/NIPAm (48.5:48.5 mol %) resulted in high nonspecific binding in both imprinted and nonimprinted polymers and a low imprinting factor of 1.1. In contrast, incorporation of 1 mol % of the negatively charged monomer methacrylic acid (MAA) with AAm/NIPAm (48.5:48.5 mol %) resulted in selective binding with an imprinting factor of 2.6, close to the value of 3.0 obtained for AAm/NIPAm (49:49 mol %) imprinted polymer.

The high level of nonspecific binding in imprinted and nonimprinted AAm/NIPAm/DMAPMA films is ascribed to electrostatic binding between the negatively charged protein ( $pI = 5.22$ ) and the positively charged (DMAPMA) side groups in the polymer. In contrast, the electrostatic repulsion between the protein and the negatively charged (MAA) side groups in AAm/NIPAm/MAA films results in much lower nonspecific binding and a higher imprinting factor (2.6). These results highlight the complexity in introducing electrostatic recognition points into imprinted polymers.

To introduce recognition points for electrostatic binding with the positively charged and negatively charged domains at the surface of MBP, we introduced monomers with both positive and negative charges into the films. The incorporation of 1% of the positively charged monomer DMAPMA and 1% of the negatively charged monomer MAA further decreases nonspecific binding. Figure 8 shows results of a binding experiment for MBP-Cy3 with an AAm/NIPAm/DMAPMA/MAA hydrogel. The hydrogel films exhibited low nonspecific binding, comparable to the films without DMAPMA and MAA, and the imprinted hydrogel exhibited high rebinding of the protein compared to the non-imprinted polymer. The imprinting factor for the AAm/NIPAm/DMAPMA/MAA hydrogel was 3.3. The imprinting factor is higher than for the AAm/NIPAm hydrogel, indicating that the monomers with charged side groups introduce additional functional groups for binding recognition, in addition to the functional groups for hydrogen bonding and hydrophobic interactions.

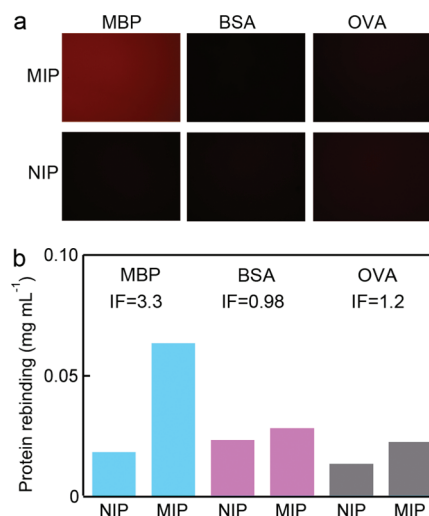


**Figure 9.** Binding of MBP, BSA, and OVA in AAm/NIPAm/DMAPMA/MAA (48%:48%:1%:1%). (a) Fluorescence images after incubation of MBP-imprinted and nonimprinted AAm/NIPAm/DMAPMA/MAA films with MBP, BSA, and OVA. (b) Protein binding for MBP and the reference proteins BSA and OVA in imprinted and nonimprinted films.

The selectivity of the AAm/NIPAm/DMAPMA/MAA hydrogel for MBP (MW 41 000,  $3 \times 4 \times 6.5$  nm,  $pI$  5.22) was investigated by performing rebinding experiments with reference proteins with similar molecular weight, dimensions, and isoelectric point. The two reference proteins are bovine serum albumin (BSA, MW 66 000,  $4 \times 4 \times 14$  nm,  $pI$  4.7) and ovalbumin (OVA, MW 45 000,  $5 \times 4.5 \times 7$  nm,  $pI$  4.6). The distribution of amino acid residues on OVA is 27% hydrophobic, 34% hydrogen bonding, 19% negatively charged, and 20% positively charged residues. In comparison to MBP, OVA has more hydrogen bonding residues and fewer charged residues. We cannot analyze the surface amino acid residues on BSA since the crystal structure is not available.

Figure 9a shows fluorescence images after incubation of imprinted and nonimprinted AAm/NIPAm/DMAPMA/MAA hydrogel films with the three proteins. The fluorescence images clearly show that the imprinted polymer binds MBP to a much larger extent than the reference proteins. Figure 9b shows the amount of protein bound to the imprinted and nonimprinted films. The selectivity of recognition is obtained from the imprinting factor, taking into account the total amount of rebinding and the amount of nonspecific binding (see eq 1). The imprinting factors were 0.98 for BSA binding and 1.2 for OVA binding, while the imprinting factor for MBP in AAm/NIPAm/DMAPMA/MAA hydrogel was 3.3. These low values reflect the fact that uptake of BSA and OVA in the MBP-imprinted films is primarily through nonspecific binding and that there is very little uptake in the MBP recognition sites, despite the similarity in physical properties.

## CONCLUSIONS

We have prepared molecularly imprinted polymer films with the ability to recognize maltose binding protein. We have developed a strategy to optimize the monomer composition for protein recognition based on analysis of the amino acid residues on the surface of the protein. MBP has solvent accessible residues available for hydrogen bonding (24%) and hydrophobic

interactions (21%) as well as negatively charged residues (22%) and positively charged residues (28%). We show that hydrogen bonding interactions, hydrophobic interactions, and electrostatic interactions can all contribute to recognition of MBP. Nonspecific binding due to electrostatic interactions can be minimized by introducing equimolar concentrations of positively and negatively charged monomers. The selectivity of the imprinted polymer films was verified in binding experiments with the reference proteins BSA and OVA.

## ■ ASSOCIATED CONTENT

**S Supporting Information.** Experimental details. This material is available free of charge via the Internet at <http://pubs.acs.org>.

## ■ AUTHOR INFORMATION

### Corresponding Author

\*E-mail: [searson@jhu.edu](mailto:searson@jhu.edu).

## ■ ACKNOWLEDGMENT

The authors gratefully acknowledge support from DTRA (Grant HDTRA1-09-0016). M.Z. thanks the Weizmann Institute of Science - National Postdoctoral Award Program for Advancing Women in Science and the Charles H. Revson Foundation for the postdoctoral fellowship support.

## ■ REFERENCES

- (1) Alexander, C.; Andersson, H. S.; Andersson, L. I.; Ansell, R. J.; Kirsch, N.; Nicholls, I. A.; O'Mahony, J.; Whitcombe, M. J. *J. Mol. Recognit.* **2006**, *19*, 106–80.
- (2) Komiyama, M. *Molecular Imprinting: From Fundamentals to Applications*; Wiley-VCH: Weinheim, 2003.
- (3) Ye, L.; Mosbach, K. *Chem. Mater.* **2008**, *20*, 859–868.
- (4) Zhang, H. Q.; Ye, L.; Mosbach, K. *J. Mol. Recognit.* **2006**, *19*, 248–259.
- (5) Haginaka, J. *Anal. Bioanal. Chem.* **2004**, *379*, 332–334.
- (6) Hilt, J. Z.; Byrne, M. E. *Adv. Drug Delivery Rev.* **2004**, *56*, 1599–1620.
- (7) Sellergren, B.; Allender, C. J. *Adv. Drug Delivery Rev.* **2005**, *57*, 1733–1741.
- (8) Byrne, M. E.; Salian, V. *Int. J. Pharm.* **2008**, *364*, 188–212.
- (9) Hoshino, Y.; Koide, H.; Urakami, T.; Kanazawa, H.; Kodama, T.; Oku, N.; Shea, K. J. *J. Am. Chem. Soc.* **2010**, *132*, 6644–+.
- (10) Hoshino, Y.; Kodama, T.; Okahata, Y.; Shea, K. J. *J. Am. Chem. Soc.* **2008**, *130*, 15242–+.
- (11) Moser, I.; Jobst, G.; Urban, G. A. *Biosens. Bioelectron.* **2002**, *17*, 297–302.
- (12) Haupt, K.; Mosbach, K. *Chem. Rev.* **2000**, *100*, 2495–2504.
- (13) Turner, N. W.; Jeans, C. W.; Brain, K. R.; Allender, C. J.; Hlady, V.; Britt, D. W. *Biotechnol. Prog.* **2006**, *22*, 1474–1489.
- (14) Hansen, D. E. *Biomaterials* **2007**, *28*, 4178–91.
- (15) Bossi, A.; Bonini, F.; Turner, A. P.; Piletsky, S. A. *Biosens. Bioelectron.* **2007**, *22*, 1131–7.
- (16) Takeuchi, T.; Hishiya, T. *Org. Biomol. Chem.* **2008**, *6*, 2459–67.
- (17) Hjerten, S.; Liao, J. L.; Nakazato, K.; Wang, Y.; Zamaratskaia, G.; Zhang, H. X. *Chromatographia* **1997**, *44*, 227–234.
- (18) Liao, J. L.; Wang, Y.; Hjerten, S. *Chromatographia* **1996**, *42*, 259–262.
- (19) El Kirat, K.; Bartkowski, M.; Haupt, K. *Biosens. Bioelectron.* **2009**, *24*, 2618–24.

- (20) Hawkins, D. M.; Trache, A.; Ellis, E. A.; Stevenson, D.; Holzenburg, A.; Meininger, G. A.; Reddy, S. M. *Biomacromolecules* **2006**, *7*, 2560–4.
- (21) Li, Y.; Yang, H. H.; You, Q. H.; Zhuang, Z. X.; Wang, X. R. *Anal. Chem.* **2006**, *78*, 317–20.
- (22) Hirayama, K.; Sakai, Y.; Kameoka, K. *J. Appl. Polym. Sci.* **2001**, *81*, 3378–3387.
- (23) Ou, S. H.; Wu, M. C.; Chou, T. C.; Liu, C. C. *Anal. Chim. Acta* **2004**, *504*, 163–166.
- (24) Kimhi, O.; Bianco-Peled, H. *Langmuir* **2007**, *23*, 6329–35.
- (25) Pang, X.; Cheng, G.; Lu, S.; Tang, E. *Anal. Bioanal. Chem.* **2006**, *384*, 225–30.
- (26) Janiak, D. S.; Ayyub, O. B.; Kofinas, P. *Macromolecules* **2009**, *42*, 1703–1709.
- (27) Hua, Z. D.; Chen, Z. Y.; Li, Y. Z.; Zhao, M. P. *Langmuir* **2008**, *24*, 5773–5780.
- (28) Kats, M.; Germain, M. E. S. *Anal. Biochem.* **2002**, *307*, 212–218.
- (29) Verheyen, E.; Schillemans, J. P.; van Wijk, M.; Demeniex, M. A.; Hennink, W. E.; van Nostrum, C. F. *Biomaterials* **2011**, *32*, 3008–20.
- (30) Crank, J. *The Mathematics of Diffusion*, 2nd ed.; Clarendon Press: Oxford, 1975.
- (31) Brass, J. M.; Higgins, C. F.; Foley, M.; Rugman, P. A.; Birmingham, J.; Garland, P. B. *J. Bacteriol.* **1986**, *165*, 787–95.
- (32) Hirokawa, Y.; Tanaka, T. *J. Chem. Phys.* **1984**, *81*, 6379–6380.
- (33) Feil, H.; Bae, Y. H.; Feijen, J.; Kim, S. W. *Macromolecules* **1993**, *26*, 2496–2500.
- (34) Schild, H. G.; Tirrell, D. A. *J. Phys. Chem.* **1990**, *94*, 4352–4356.